

CHAPTER 7

*Radiation Effects on Matter**

Contents

7.1.	Energy transfer	167
	7.1.1. Charged particles	167
	7.1.2. Uncharged radiation	169
7.2.	Radiation tracks	169
7.3.	Radiation dose and radiation yield	170
7.4.	Metals	172
7.5.	Inorganic nonmetallic compounds	173
7.6.	Water	176
7.7.	Aqueous solutions	177
7.8.	Organic compounds	180
7.9.	Experimental methods	183
7.10.	Dose measurements	184
7.11.	Large-scale non-biological applications	186
	7.11.1. Radiation sources	187
	7.11.2. Process criteria	187
	7.11.3. Radiation induced synthesis	188
	7.11.4. Industrial radiation processing	189
7.12.	Technical uses of small dose-rates	189
7.13.	Exercises	190
7.14.	Literature	190

Soon after the discoveries of X-rays and radioactivity it was learned that radiation could cause changes in matter. In 1901 P. Curie found that when a radium source was placed on his skin, wounds were produced that were difficult to heal. In 1902 skin cancer was shown to be caused by the radioactivity from radium but 5 years later it was learnt that radium therapy could be used to heal the disease. Large radiation doses were found to kill fungi and microorganisms and produce mutations in plants.

Glass ampules containing milligrams of radium darkened within a few months and became severely cracked, allowing the leakage of radon gas. In the early years of the investigation of radioactivity, emphasis was on radium and its decay products. Among the radiation effects observed were the fluorescence induced in different salts and the changes in their crystallographic form. Metals were found to lose their elasticity and become brittle. Radiation was also found to have a profound effect on the chemical composition of solutions and gases. Water, ammonia and simple organic substances decomposed into more

* This chapter has been revised by Prof. T. Eriksen, Royal Institute of Technology, Stockholm

elementary constituents and also combined into more complex polymeric products. Radiation decomposition (*radiolysis*) of water caused evolution of hydrogen and oxygen gas and formation of hydrogen peroxide. Conversely, it was shown that water could be synthesized through irradiation of a mixture of H₂ and O₂. In 1911 S. Lind found that 1 g of radium exposed to air resulted in the production of 0.7 g of ozone per hour. By relating this *radiation yield* to the number of ions produced by the amount of radiation, Lind initiated the quantitative treatment of radiation-induced changes.

7.1. Energy transfer

The chemical effects of radiation depends on the composition of matter and the amount of energy deposited by the radiation. In this section we consider only the energy transfer. For this purpose it is practical to divide high energy radiation into (1) charged particles (e⁻, e⁺, α, etc) and (2) uncharged particles (n) and electromagnetic radiation (γ). The latter produce recoil atomic ions, products of nuclear reactions and electrons as charged secondary ionizing particles. The terms direct and indirect ionizing radiation are often used for (1) and (2) respectively.

The amount of energy imparted to matter in a given volume is

$$E_{\text{imp}} = E_{\text{in}} + \Sigma Q - E_{\text{out}} \quad (7.1)$$

where E_{in} is the energy (excluding mass energy) of the radiation entering the volume, E_{out} is the energy of the radiation leaving the volume, ΣQ is the sum of all Q -values for nuclear transformation that have occurred in the volume. For a beam of charged particles $E_{\text{in}} = E_{\text{kin}}$; for γ -rays it is E_{γ} . If no nuclear transformations occur, $\Sigma Q = 0$. For neutrons which are captured and for radionuclides which decay in the absorber, $\Sigma Q > 0$; in the case of radionuclides already present in the absorber, $E_{\text{in}} = 0$.

7.1.1. Charged particles

We learned in the previous chapter that the energy of charged particles is absorbed mainly through ionization and atomic excitation. For positrons the annihilation process (at $E_{\text{kin}} \approx 0$) must be considered. For electrons of high kinetic energy bremsstrahlung must be taken into account. However, in the following we simplify by neglecting annihilation and bremsstrahlung processes. The bremsstrahlung correction can be made with the aid of Figure 6.9 which gives the *average specific energy loss* of electrons through ionization and bremsstrahlung.

It has been found that the average energy w for the formation of an ion pair in gaseous material by charged particles is between 25 and 40 eV. For the same absorbing material it is fairly independent of the type of radiation and the energy. Table 7.1 lists values of w in some gases. The ionization potentials j of the gases are lower than the w -values and the rest of the energy, $w-j$, must be used for excitation. Since the excitation energies per atom are ≤ 5 eV, several excited atoms are formed for each ion pair formed. While it is easy to measure w in a gas, it is more difficult to obtain reliable values for liquids and solids. They also differ more widely; e.g. w is 1300 eV per ion pair in hexane (for high energy

Table 7.1. Ion pair formation energies for charged particles. All values in eV.

Absorber	w	j	$w \cdot j$
He(g)	43	24.5	18.5
H ₂ (g)	36	15.6	20.4
O ₂ (g)	31.5	12.5	19
Air	34	15	19
H ₂ O(g or l)	38	13	25
Ar(g) 5 MeV α	26.4		
Ar(g) 340 MeV p	25.5		
Ar(g) 10 keV e ⁻	26.4		
Ar(g) 1 MeV e ⁻	25.5		
Ar(g) average	26	15.7	10.3

electrons) while it is about 5 eV per ion pair in inorganic solids.

The *specific energy loss* of a particle in matter is called the *stopping power* \hat{S} ,

$$\hat{S} = dE_{\text{loss}}/dx \text{ (J/m)} \quad (7.2)$$

where x is the distance traversed by the particle. To a good first approximation the stopping power of a material is determined by its atomic composition and is almost independent of the chemical binding of the atoms. Stopping power is a function of the particle velocity and changes as the particle is slowed down.

The *specific ionization* J is the number of ion pairs produced per unit path length

$$J = dN_i/dx \text{ (ion pairs/m)} \quad (7.3)$$

The value of J depends on the particle and its energy as seen from Figure 6.7. The relation between \hat{S} and J is

$$\hat{S} = w J \text{ (J/m)} \quad (7.4)$$

The *mass stopping power*, \hat{S}/ρ , is commonly expressed in units of MeV/g cm².

Another important concept is the *linear energy transfer* (abbreviated as *LET*) of charged particles. It is defined as the energy absorbed in matter per unit path length traveled by a charged particle

$$LET = dE_{\text{abs}}/dx \quad (7.5)$$

Values of *LET* in water are given for various particles and energies in Table 6.2. For the same energy and the same absorbing material, the *LET* values increase in the order:

- ↓ high energy electrons (also approximately γ -rays)
- ↓ β -particles (also approximately soft X-rays)
- ↓ protons
- ↓ deuterons
- ↓ α -particles
- ↓ heavy ions (ions of N, O, etc.)
- ↓ fission fragments

The relationship between *LET*, which refers to the energy absorbed in matter, and the stopping power, which refers to the energy loss of the particle, is

$$dE_{\text{loss}}/dx = dE_{\text{abs}}/dx + E_x \quad (7.6)$$

The difference E_x in these two energy terms is related to the energy loss by electromagnetic radiation (mainly bremsstrahlung).

7.1.2. Uncharged radiation

When neutrons or photons having the incident particle energy E_{in} are absorbed, a certain fraction of energy E_{tr} is transferred into kinetic energy of charged particles when traversing the distance dx . We can define an *energy transfer coefficient* as

$$\mu_{\text{tr}} = E_{\text{in}}^{-1} dE_{\text{tr}}/dx \quad (\text{m}^{-1}) \quad (7.7a)$$

If we neglect the bremsstrahlung associated with the absorption of the secondary charged particles formed in the initial absorption processes, E_{tr} is the energy absorbed (designated as E_{abs}), and we can write (7.7a) as

$$\mu_{\text{a}} = E_{\text{in}}^{-1} dE_{\text{abs}}/dx \quad (\text{m}^{-1}) \quad (7.7b)$$

7.2. Radiation tracks

The energy lost when a high energy charged particle is slowed in matter gives rise to a trail (or, more commonly, track) of ionized and excited molecules along the path of the particle; Figure 7.1 schematically depicts a track. Figure 6.5 shows cloud chamber photographs of such tracks. A photon imparts a large fraction of its energy to a single electron which subsequently ionizes and excites many other molecules along its path. The absorption of any type of ionizing radiation by matter thus leads to the formation of tracks of ionized and excited species. Whereas these species generally are the same in a particular sample of matter regardless of the type of radiation, the tracks may be sparsely or densely populated by these species. Expressions such as linear energy transfer (*LET*) and stopping power (\dot{S}) are based on the implicit assumption of a continuous slowing down process and thus gives quantitative information on the average energy loss but only qualitative information on the densities of reactive species.

Electrons are liberated in the ionization process with greatly varying kinetic energy. If the energy of these secondary electrons is relatively low (< 100 eV) their range in liquids and solids is short and the ionizations and excitations caused by these electrons take place close to the primary ionizations leading to the formation of small *spurs* containing ionized and excited species. Secondary electrons with high kinetic energy form tracks of their own branching from the primary track. Such electrons are called δ -rays. For high energy electrons spurs are formed at well separated intervals along the track whereas for densely ionizing radiation such as α particles, protons and recoil atomic ions the spurs overlap and form

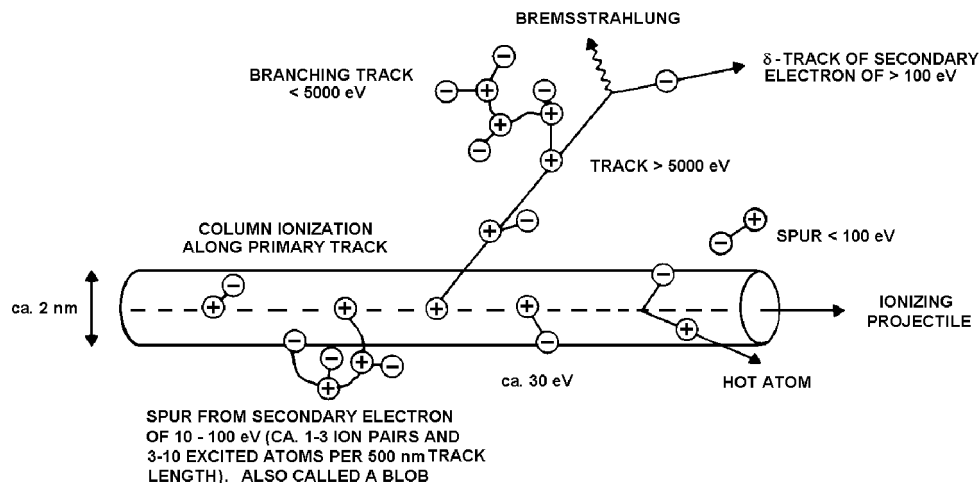


FIG. 7.1. Track formed by energetic ionizing particle in condensed matter. Distances between ion pairs along track are: ~ 1000 nm γ , 500-100 nm fast electron, ~ 1 nm slow electron and α .

columns of excited and ionized species. Differences in chemical and biological effects caused by different radiations reflects the varying track structures.

The tracks of X-ray and γ -radiation results in tracks of fast electrons. The energy of these fast electron is consumed by the formation of spurs (6 – 100 eV), blobs (100 – 500 eV) and short tracks (500 – 5000 eV), see Figure 7.1. For a primary electron in the range $10^4 - 10^7$ eV the distribution of energy of secondary electrons is approximately 40% < 3.4 eV, 20% 3.4 – 6.8 eV, 18% 6.8 – 13.5 eV and 12% 13.5 – 27.1 eV. The radius of the core at low electron velocities is of the order of 1 nm.

The energy transferred to the electrons by an energetic ion depends on the mass, the charge (Z) and velocity (v) of the ion, cf. (6.13): the probability of interaction is proportional to the ratio Z^2/mv^2 . Heavy ions produce track structures similar to those of fast electrons. However, the spurs are quite close to each other and, for the case of α -particles, the original distance between them is of the order of fractions of a nanometer. Immediately at their formation they comprise a continuous cylindrical column. The column consists of a dense core surrounded by a more diffuse shell of tracks of high energy δ -electrons.

7.3. Radiation dose and radiation yield

The oldest radiation unit still in use is the *roentgen* (R). It applies only to photons and is defined as the *exposure*. The exposure is the energy flux of the unperturbed photon radiation hitting matter. 1 R is the exposure that in air produces ion pairs with total charge per unit mass of 2.58×10^{-4} C/kg. This corresponds to 1.61×10^{15} ion pairs per kg air or 8.8×10^{-3} J/kg absorbed energy at an average ion pair formation energy of 34 eV. The roentgen has been in use for more than 60 years and is still not uncommon in the medical profession.

The *absorbed dose* (D) is the amount of radiation energy absorbed per unit mass:

$$D = dE_{\text{abs}}/dm \quad (7.8)$$

According to (7.1) $E_{\text{abs}} = E_{\text{in}} - E_{\text{out}}$. The SI unit is the *Gray* (Gy)

$$1 \text{ Gy} = 1 \text{ J/kg}$$

An old, still sometimes used, unit is the *rad* (for radiation absorbed dose)

$$1 \text{ Gy} = 100 \text{ rad}$$

The *dose rate* is the absorbed dose per unit time. The SI unit is Gray per second (Gy/s).

The *specific γ -ray dose rate*, \mathcal{D} , is a practical measure for estimation of the radiation hazard to people from γ -emitting radionuclides:

$$\mathcal{D} = A r^{-2} \sum n_i k_i B_i e^{-\mu_i x} \quad (7.9)$$

where $A r^{-2} \sum n_i k_i = \mathcal{D}_0$ is the relative dose rate (Gy/s) without any radiation shielding, and \mathcal{D} the same for a radiation shield with build-up factor B_i and attenuation factor $e^{-\mu_i x}$ (see eqns. 6.26 – 6.27); n_i is the fraction of all decays (given by the decay scheme of the source nuclide) yielding a γ -ray of energy E_i corresponding to the source constant k_i

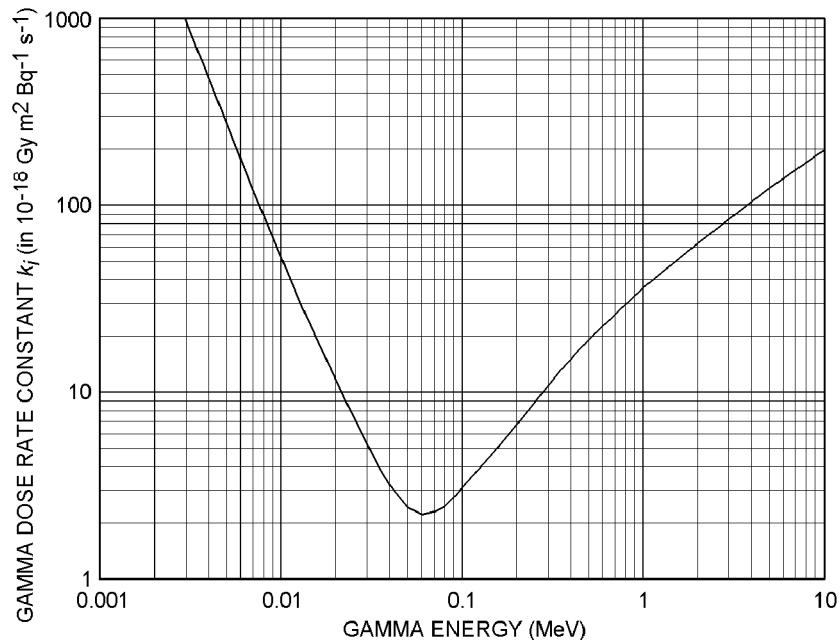


FIG. 7.2. Dose rate constant for a monoenergetic point isotropic γ -source as a function of γ -energy.

according to Figure 7.2, and A is the source strength (Bq). E.g. ^{24}Ne decays (Fig. 4.6) to 8% with two γ 's (0.878 and 0.472 MeV) and to 92% with one γ (0.472 MeV). Thus the sum in (7.9) contains two terms, one for 0.878 MeV γ ($n_1 = 0.08$) and one for 0.472 MeV γ ($n_2 = 1$). The k_i -values are taken from Figure 7.2. The relaxation length $\mu_i x$ is computed for each energy E_i and the corresponding attenuation factors of the radiation shield $e^{-\mu_i x}$ (x m thick) are calculated using e.g. Figure 6.17. Build-up factors B_i can be estimated from Figure 6.20. It should be noted that (7.9) does not account for scattering around the shield ("sky-shine"), which has to be estimated separately; see text books on radiation shielding.

Closely related to the absorbed dose is the *kerma* (K), which is the kinetic energy released per unit mass by uncharged particles and electromagnetic radiation (n and γ):

$$K = dE_{tr}/dm = \phi E \mu_{tr} \rho^{-1} \quad (7.10)$$

where E is the radiation energy, ϕ is the particle fluence (particles/m²) and μ_{tr}/ρ is the mass energy transfer coefficient. The SI unit of the kerma is J/kg.

In the following we refer to all absorbed radiation energy as the radiation dose independent of whether the incident radiation is charged or uncharged particles or photons.

Radiation chemical yield is described in terms of *G-values*. Originally $G(x)$ was defined as the number of molecules of x transformed per 100 eV absorbed energy (a practical notation as most reactions have G -values of < 10). In the SI system the symbol $G(x)$ is the same but the unit is mol/J. The conversion factor between the two units is $1 \text{ mol/J} = 9.649 \times 10^6$ molecules per 100 eV absorbed.

7.4. Metals

Metals consist of a solid lattice of atoms whose valence electrons cannot be considered to belong to any particular atom, but rather to a partially filled energy band (the conduction band) established by the total lattice network. Interaction of radiation with the metal can cause *excitation* of bound electrons in the atoms to the conduction band.

While irradiation by γ -rays and electrons has little influence on metallic properties, heavy particles cause serious damage through their collision with atoms in the metal lattice network. This results in *displacements* of the atoms from their lattice positions. The number of displacements (n_{disp}) depends on the amount of energy transferred in the collision event (E_{tr}) to the recoiling (target) atom, and the energy required for moving this atom from its lattice position. This so-called *displacement energy* (E_{disp}) is 10 – 30 eV for most metallic materials. According to the Kinchin-Pease rule,

$$n_{\text{disp}} \leq E_{tr}/(2 E_{\text{disp}}) \quad (7.11)$$

The maximum energy transferred can be calculated assuming purely elastic collisions between hard spheres (§12.1). Thus for a 1.5 MeV fission neutron, $E_{tr}(\text{max})$ is 425 keV in C, 104 keV in Fe, and 25 keV in U. With $E_{\text{disp}} \approx 25$ eV, up to 8500, 2080 and 500 displacements, respectively, occur in these metals due to the absorption of a fission neutron (neglecting nuclear reactions). In practice the numbers are somewhat smaller, especially at

the higher E_{tr} (where it may be about one third of the calculated value). Atomic displacements cause many changes in the properties of metals. Usually electrical resistance, volume, hardness and tensile strength increase, while density and ductility decrease.

The microcrystalline properties of metals are particularly influenced by irradiation. Although low-alloy steel in modern reactor tanks are rather radiation resistant (provided they are free of Cu, P and S impurities), stainless steel (e.g. of the 18% Cr, 8% Ni type) has been found to become brittle upon irradiation due to the formation of microscopic helium bubbles, probably due to n, α reactions in ^{54}Fe and impurities of light elements (N, B, etc.). This behavior is accentuated for metallic uranium in reactors because of the formation of fission products, some of which are gases. As a result of this radiation effect it is not possible to use uranium metal in modern power reactors, where high radiation doses are accumulated in a very short time. The fuel elements for power reactors are therefore made of nonmetallic uranium compounds.

The displaced atoms may return to their original lattice positions through diffusion if they are not trapped in energy wells requiring some activation energy for release. Such energy can be provided by heating or by irradiation with electrons or γ -rays (these do not cause new displacements). This "healing" of particle radiation damage is commonly referred to as annealing. The *thermal annealing rate* increases with temperature as does *radiation annealing* with radiation dose. Doses in the 10 kGy range are usually required for appreciable effect.

7.5. Inorganic nonmetallic compounds

The time for a high energy particle to pass by an atom is $\leq 10^{-16}$ s. In this time the atom may become excited and/or ionized, but it does not change position (the *Franck-Condon principle*) provided there is no direct collision. The excited atoms are de-excited through the emission of *fluorescence radiation*, usually within 10^{-8} s. The ionization can result in simple trapping of the electrons and production of "electron holes" in the lattice, especially at impurity sites. The local excess (or deficiency) of charge produced in this way leads to electronic states with absorption bands in the visible and ultraviolet regions of the spectrum. For example, irradiation of LiCl results in a change of the color of the compound from white to yellow. Similarly, LiF becomes black, KCl blue, etc. The irradiation of ionic crystals also leads to changes in other physical properties such as conductivity, hardness, strength, etc. Frequently, heating returns the properties and color to the normal state (or close to it) accompanied by the emission of light; this forms the basis for a radiation dose measurement technique named "thermoluminescence dosimetry" (§8.9).

Following a collision between a heavy particle (n, p, etc.) and an absorber atom in a crystalline material the recoiling ion produces lattice vacancies and, upon stopping, may occupy a non-equilibrium interstitial position (Fig. 7.3). The localized dissipation of energy can result in lattice oscillations, terminating in some reorientation of the local regions in the crystal lattice. These crystal defects increase the energy content of the crystal. Semiconductors, where the concentration of charge carriers is very small, have their conductivity reduced by introduction of lattice defects during irradiation. The production of interstitial atoms makes the graphite moderator in nuclear reactors stronger, harder, and more brittle. Since these dislocated atoms are more energetic than the atoms in the lattice,

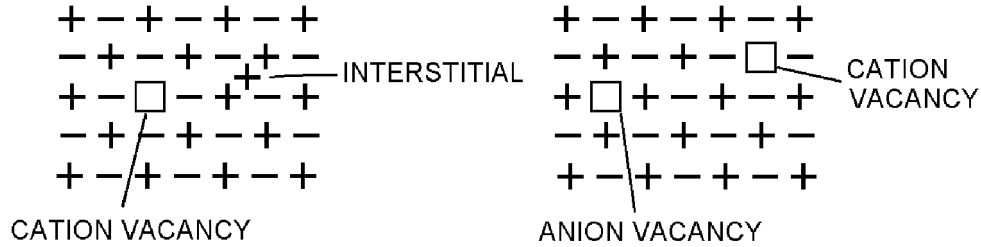
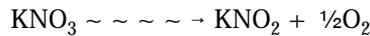


FIG. 7.3. Irradiated NaCl type crystal showing negative and positive ion vacancies.

the dislocations lead to an energy storage in the material (the *Wigner effect*), which can become quite significant. For reactor graphite at 30°C this frequently reaches values as high as 2000 kJ/kg for fluencies of 2×10^{21} n/cm². At room temperature the interstitial atoms return to their normal positions very slowly (annealing), but this rate is quite temperature dependent. If the elimination of the interstitial atoms occurs too rapidly, the release of the Wigner energy can cause the material to heat to the ignition point. This was the origin of a fire which occurred in a graphite moderated reactor in England in 1957, in which considerable amounts of radioactive fission products were released into the environment.

Inorganic substances exposed to high fluencies of neutron and γ -radiation in nuclear reactors are found to experience decomposition. Thus:



The notation $\sim \sim \sim \sim \rightarrow$ symbolizes a radiation induced reaction. At high fluxes the oxygen pressure in the KNO_3 causes the crystal to shatter. However, some crystals are remarkably stable (although they may become colored), e.g. Li_2SO_4 , K_2SO_4 , KCrO_4 , and CaCO_3 .

Theory has not been developed sufficiently to allow quantitative calculation of the radiation sensitivity of compounds. Usually covalent binary compounds are highly radiation

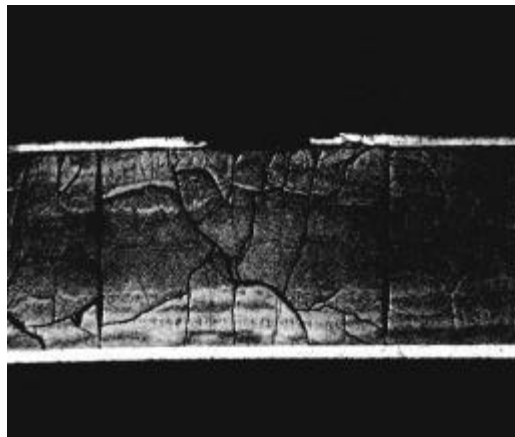


FIG. 7.4. Zircaloy canned UO_2 fuel after exposure to very high power (high dose and heat) in test reactor. The pellets have fractured and the canning has been penetrated. (SKI report)

resistant. Two examples are UO_2 and UC , whose insensitivity to radiation has led to their use as reactor fuels. In the fuel elements of commercial water cooled reactors UO_2 is used in the form of small, sintered pellets about 1 cm^3 in volume. Because of the build-up of pressure from fission gases, these pellets crack at high fluxes ($\geq 10^{22} \text{ n/cm}^2$); Figure 7.4. Another binary compound, CO_2 , which is used as a coolant in some older reactors, decomposes by irradiation to graphite and polymeric species.

In mixtures of inorganic compounds many unexpected and even undesirable reactions may occur. For example, radiolysis of liquid air (often used in radiation research) yields ozone, while radiation of humid air yields HNO_3 . One of the first observations of radiation-induced changes was the darkening of glass. Glass often contains iron, manganese, and other metals that can exist in several oxidation states with different colors. As a result of the irradiation, the oxidation state can change, resulting in change in color. Dislocations as well as trapped electrons also contribute to the color changes in glass. In chemical and metallurgical work with highly active substances it is desirable to observe the experiment through a thick glass window, which provides protection from the radiation. In order to avoid the coloring of the glass, a small amount (1 - 2%) of an element which can act as an electron trap is added, e.g. CeO_2 , which acts by the reaction $\text{Ce}^{4+} + \text{e}^- \rightarrow \text{Ce}^{3+}$. After an exposure of 10^4 Gy the transmission to light of ordinary glass had been reduced to 44%, while for a CeO_2 protected glass it was still 89%.

Glass is very resistant to radiation damage because it is a noncrystalline solid liquid. Therefore, in such a material, it is not possible to speak of dislocations: the random structure of the glass allows it to include foreign species throughout the sample. This is why glass has been intensely studied, including full scale tests, as the matrix ("container") for high active waste (HAW) consisting of fission products and actinides.

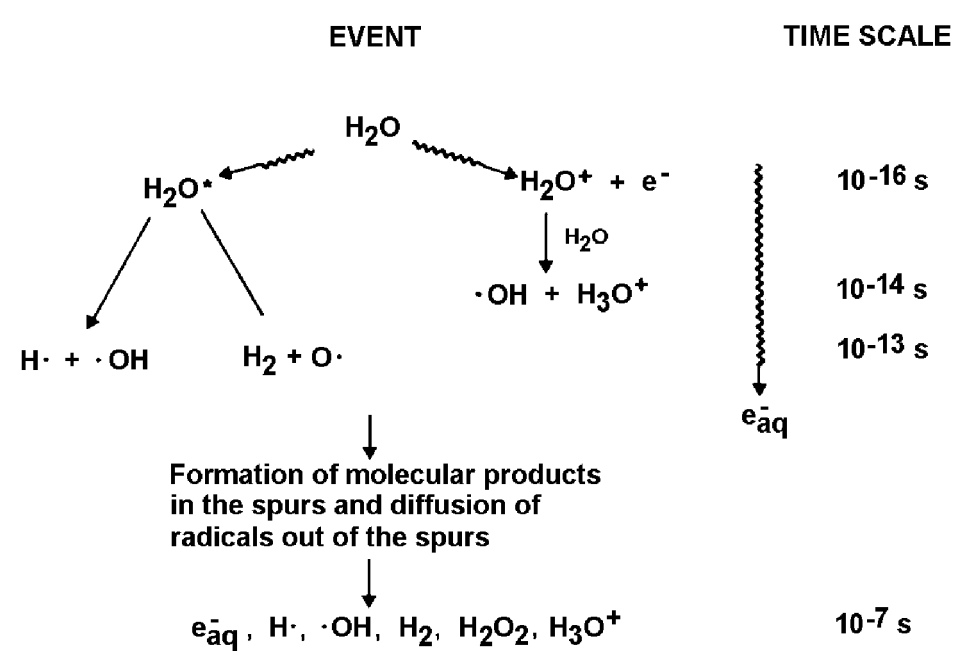


FIG. 7.5. Time scale of radiolysis of water.

Table 7.2. Spur reactions in water

$e_{\text{aq}}^- + e_{\text{aq}}^- \rightarrow \text{H}_2 + 2\text{OH}^-$
$e_{\text{aq}}^- + \cdot\text{OH} \rightarrow \text{OH}^-$
$e_{\text{aq}}^- + \text{H}_3\text{O}^+ \rightarrow \text{H}\cdot + \text{H}_2\text{O}$
$e_{\text{aq}}^- + \text{H}\cdot \rightarrow \text{H}_2 + \text{OH}^-$
$\text{H}\cdot + \text{H}\cdot \rightarrow \text{H}_2$
$\cdot\text{OH} + \cdot\text{OH} \rightarrow \text{H}_2\text{O}_2$
$\cdot\text{OH} + \text{H}\cdot \rightarrow \text{H}_2\text{O}$
$\text{H}_3\text{O}^+ + \text{OH}^- \rightarrow \text{H}_2\text{O}$

7.6. Water

The consequences of ionization and excitation depend on the physical state and the molecular composition of the irradiated material. In this section we introduce chemical phenomena into the description using the radiolysis of water as an example.

The time scale for the sequence of events on the radiolysis of water is shown in Figure 7.5. The ionization event occurs on the time scale of an electronic transition ($< 10^{-16}$ s). The positive ion H_2O^+ formed reacts with water within 10^{-14} s, forming an $\cdot\text{OH}$ radical and H_3O^+ . The electron, if liberated with sufficient kinetic energy, can ionize further water molecules before its energy falls below the ionization threshold of water (12.61 eV). The electron thereafter loses the rest of its energy by causing vibrational and rotational excitation of the water molecules and, finally, becomes solvated.

The solvation process has been shown to occur within 10^{-12} s. The excited states dissociate within $10^{-14} - 10^{-13}$ s, i.e. on the same time scale as a molecular vibration to form $\text{O}\cdot$, $\text{H}\cdot$, $\cdot\text{OH}$ and H_2 . The physical and physicochemical (pre-thermal) processes are thus completed within 10^{-12} s leaving the species in thermal equilibrium with the water.

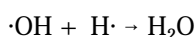
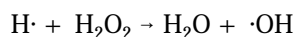
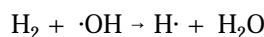
The radiolysis products are clustered in spurs (Fig. 7.1); i.e., they are inhomogeneously distributed in the water and proceed to diffuse out of the spur volume. During this "spur diffusion" process, recombination reactions take place leading to the formation of molecular or secondary radical products. The spur expansion is complete within 10^{-7} s, at which time the radiolysis products are those shown in Figure 7.5. Spur reactions are listed in Table 7.2. *G*-values for the radiolysis products in water irradiated with different types of radiation are given in Table 7.3. It is seen that, as the *LET* of the radiation increases, the *G*-values

Table 7.3. Product yields ($\mu\text{mol/J}$) in irradiated neutral water

Radiation	$G(-\text{H}_2\text{O})$	$G(\text{H}_2)$	$G(\text{H}_2\text{O}_2)$	$G(e_{\text{aq}}^-)$	$G(\text{H}\cdot)$	$G(\cdot\text{OH})$	$G(\cdot\text{HO}_2)$
Liquid water:							
γ and fast electrons	0.43	0.047	0.073	0.28	0.062	0.28	0.0027
12 MeV He^{2+}	0.294	0.115	0.112	0.0044	0.028	0.056	0.007
Water vapor:							
γ , electrons	0.85	0.05	0	$G(e^-) = 0.31$	0.75	0.85	

of radical products decrease while the molecular G -values increase, which evidences the formation of tracks. The higher G -values for water consumption and for molecular product formation in irradiated water vapor, as compared to liquid water, show that spur formation and spur reactions are of minor importance in the vapor phase. This is to be expected in a less dense medium where the average distance between separate spurs will be larger. Also the diffusivities will be larger in the vapor phase.

In the absence of solutes, reactions between radical and molecular species occur in the bulk water. In pure water irradiated with γ or X -rays, water is reformed via the reactions



and no net decomposition of water is observed. The yields depend on the LET -value of the radiation, as illustrated in Figure 7.6 for acidic and neutral water. Irradiation with higher LET radiation, which have higher G -values for molecular than for radical products, causes net decomposition of water.

In nuclear reactors water used as a coolant or moderator should be as pure as possible to minimize dissociation during the time in the reactor. The formation of an explosive gas mixture of H_2 and O_2 must be carefully avoided in all reactors in order to prevent accidents. Moreover the decomposition products of water can increase the corrosion of fuel elements, structural material, etc. Many reactors use N_2 as a protective gas. In this case the radiolysis can lead to the formation of HNO_3 unless suppressed by an excess of H_2 which preferentially yields NH_3 . The pH of the water may be regulated by the $\text{H}_2(\text{g})$ pressure.

7.7. Aqueous solutions

In irradiated dilute aqueous solutions at concentrations < 0.1 mol/l, practically all the energy absorbed is deposited in the water molecules. Hence, the observed chemical changes are the result of the reactions between the solutes and the products of the water radiolysis. With increasing solute concentrations, the direct radiolysis of the solute gradually becomes important and the solute may also interfere with the spur reactions. The use of high concentrations of solutes which react selectively with the radical products -- so-called *scavengers* -- have provided experimental support for the existence of spurs.

In dilute solutions the chemical changes of a specific solute primarily reflect its reactivity towards e_{aq}^- , $\text{H}\cdot$ and $\cdot\text{OH}$. The hydrated electron e_{aq}^- is a strongly reducing species ($E_0 = -2.9$ V) whereas the hydrogen atom is a less powerful reductant ($E_0 = -2.3$ V). The H atom can be considered as a weak acid with a pKa of 9.6



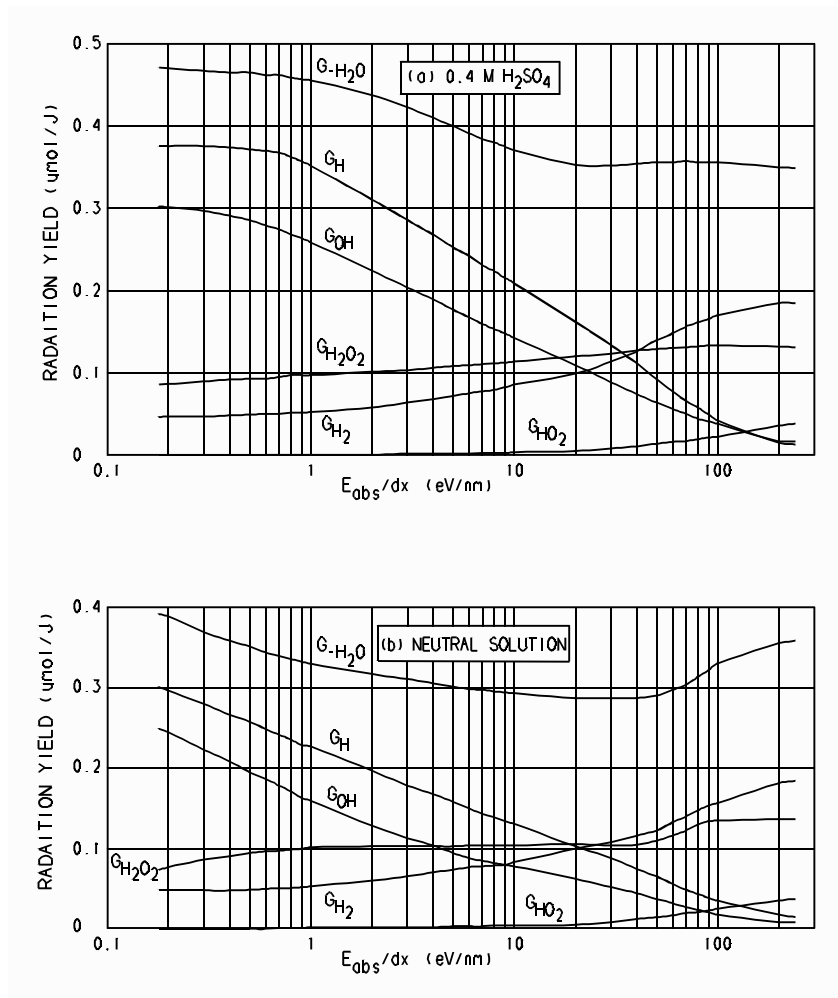
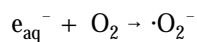


FIG. 7.6. G -values ($\mu\text{mol/J}$) for radiolysis of water as a function of the LET value (eV/nm) of the system: (a) $0.4 \text{ M H}_2\text{SO}_4$, and (b) neutral solution. (From A. O. Allen.)

The hydroxyl radical $\cdot\text{OH}$ is a strong oxidant ($E_0 = 2.7 \text{ V}$ in acidic and 1.8 V in basic solution). In strongly alkaline solution $\cdot\text{OH}$ dissociates into its anionic form O^- which has nucleophilic properties



In oxygenated solutions the perhydroxyl radical $\cdot\text{HO}_2$ is formed in reactions between e_{aq}^- , $\cdot\text{H}$ and O_2



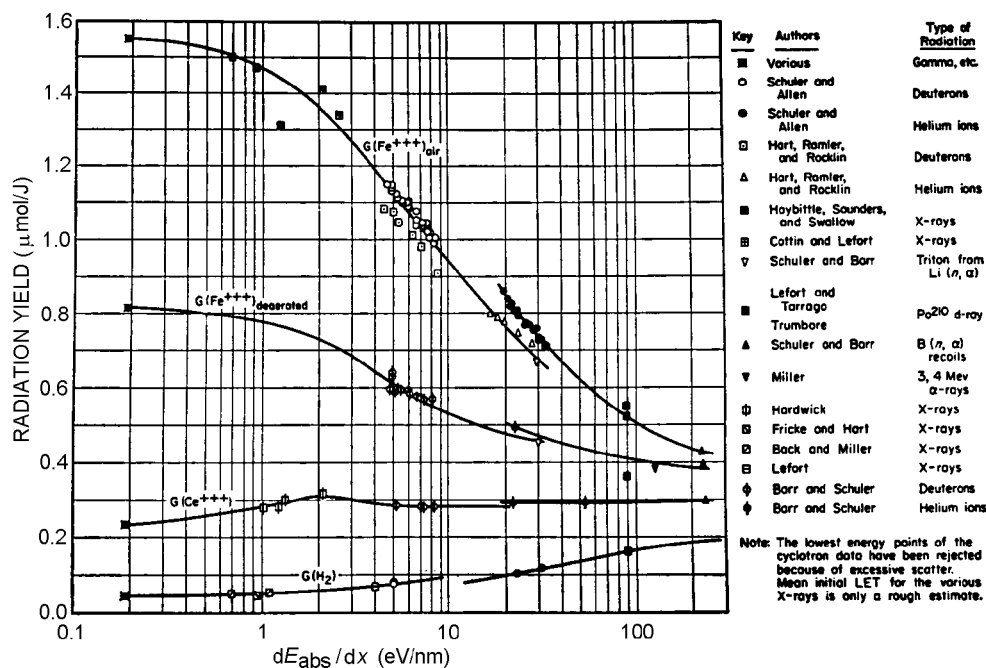
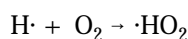
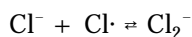
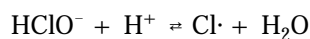


FIG. 7.7. Radiation yield for oxidation of Fe^{2+} and reduction of Ce^{4+} in slightly acid (H_2SO_4) solution as a function of the radiation LET value. (From A. O. Allen.)



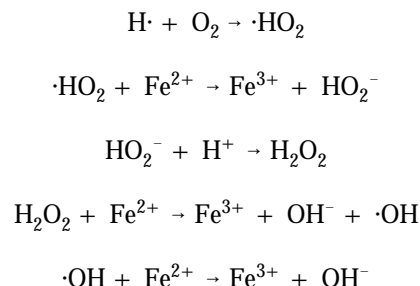
In saline waters (0.1 M Cl^- , pH 4 – 10) the dominant radiolysis reactions are



These equilibria are pH-dependent, and the reactions may have important consequences for storage of nuclear waste in salt media.

The oxidation of Fe^{2+} to Fe^{3+} in acidic oxygenated solution is the basis for the *Fricke dosimeter*, §7.10. The reaction scheme is:





The yield of Fe^{3+} is given by the equation

$$G(\text{Fe}^{3+}) = 2G(\text{H}_2\text{O}_2) + 3[G(\text{e}_{\text{aq}}^-) + G(\cdot\text{H}) + G(\cdot\text{HO}_2)] + G(\cdot\text{OH}) \quad (7.12)$$

Figure 7.7 shows radiation yields for oxidation of Fe^{2+} in acidic solution as a function of the *LET* value (see also §7.10).

When the concentration of the aqueous solution is greater than ≈ 0.1 M, the solutes may undergo direct radiolysis. The products of the radiolysis of the solute can react with water itself or with the radiolytic products of water. Irradiation of solutions containing sulfate, sulfite, or sulfide ions with *fast neutrons* yields radioactive phosphorus, through the $^{32}\text{S}(\text{n},\text{p})^{32}\text{P}$ reaction, almost exclusively as orthophosphate. However, depending on the redox conditions of the solution, reduced species of phosphorus also appear in minor amounts. Somewhat in contrast to this, *slow neutron* irradiation of solutions of NaHPO_4 yields phosphorus in many different oxidation states; thus P(+1), P(+3) and P(+5) appear in species such as hypophosphite, phosphite, and o-phosphate. These species are all rather stable in aqueous solutions, and have been identified through paper electrophoretic analysis. In general, it may be assumed that slow neutron irradiation of solutions of oxyanions changes the central atom to another (usually a more reduced) valence state through n,y-reactions. For example, while manganese is in the Mn(+7) state in MnO_4^- , neutron capture leads to the formation of $^{56}\text{Mn}^{2+}$ species. However, if the product valence state is unstable at ambient solution conditions, it may be immediately oxidized to a more stable higher valence state.

The *self radiolysis* of a solution may change the chemical equilibria of the solution components. For example, the α -decay of plutonium decomposes water; in a solution containing 1 mole of ^{239}Pu , ca. 0.01 mole of H_2O_2 is produced per day. This hydrogen peroxide can react with the plutonium to form a precipitate of plutonium peroxide. To avoid this precipitation, nitrite ions are added to the solution to react with the hydroxyl radicals formed by the radiolysis and to eliminate the H_2O_2 .

7.8. Organic compounds

As discussed above, the chemical consequences of radiolysis depends on the physical state and the molecular composition of the irradiated material. Two properties, the dielectric constant and the electron mobility, are of great importance for the fate of the ion pairs (the radical cations and the electrons) formed on ionization.

Table 7.4. Onsager radii, electron mobilities and free ion yields

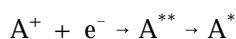
Liquid	r_c (nm)	mobility ($\text{cm}^2/\text{V s}$)	$G(\text{free ions})$ ($\mu\text{mol/J}$)
Neopentane	32	55	0.09 – 0.11
Cyclohexane	28	0.35	0.016 – 0.02
Benzene	25	-	0.005 – 0.008
Methanol	2.3	-	0.2
Water	0.7	-	0.28

The distance r_c (the *Onsager radius*) at which the potential energy of an ion pair corresponds to the thermal energy kT is, according to Onsager,

$$r_c = e^2 / 4\pi \epsilon_0 \epsilon_r k T \quad (7.13)$$

where ϵ_0 and ϵ_r is the permittivity of free space and in the medium at distance r_c , respectively (the *Onsager equation*). The probability of an electron escaping its positive ion to become a free ion is equal to $e^{-r_c/r}$ (r is the distance travelled by the electron before it becomes thermalized) depends on the electron mobility in the medium. Most organic liquids have a lower dielectric constant than that of water and the free ion yields are, therefore, generally lower, see Table 7.4.

Electrons escaping their positive ions are gradually thermalized and solvated whereas electrons that recombine with their geminate (i.e. original ion pair) radical cations form excited molecules. The radical cations may react with solvent molecules. The types of reactions to be expected are e.g. proton, hydrogen atom and hydride ion transfer. Excited molecules are thus formed directly and by geminate ion recombination



The highly excited (electronically and/or vibrationally) molecule A^{**} formed by charge recombination may (within 10^{-11} s) lose part of its energy rapidly through collisions with its neighboring molecules. The excited molecules can return to their ground state by several processes. *Singlet states* (antiparallel spins of valence electrons) de-excite within 10^{-8} s by *fluorescence*, whereas the *phosphorescence* of *triplet states* (parallel spins of the outer electrons) requires 10^{-5} to 10 s. Alternatively the excited molecules can undergo unimolecular isomerization reactions or dissociate into highly reactive radicals.

Organic molecules in general have more atoms than water and, therefore, the formation of a higher variety of products is to be expected. Both molecules smaller than the original and polymeric products are formed.

The effects of radiation on organic molecules have been shown to be strongly dependent on the molecular structure. Since the excitation energy is rapidly spread out over the whole molecule, one would expect the weakest bond to rupture, producing two radicals, provided

Table 7.5. Effects of γ -radiation on organic compounds of technical interest

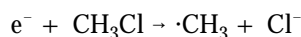
Compound	Observed change at (kGy)	Useless at (kGy)	Compound	25% reduction of desired property (kGy)
Olefins	5	10	Teflon	0.1
Silicones	5	50	Cellulose acetate	2
Mineral oils	10	100	Polyethylene	9
Alkyl aromatics	100	500	Polyvinylchloride	10
Polyphenyls	500	5000	Polystyrene	400
			Neoprene, silicon rubber	0.6
			Natural rubber	2.5

the excitation energy exceeds the bond energy. Typical bond energies are C-C \leq 3.9, C=C (aliph) 6.4, C=C (arom) 8.4, C \equiv C \leq 10, C-H 3.5 - 4.5, C-O 3.7 and C=O 7.7 eV. Although C-C bonds are weaker than C-H bonds, C-H rupture predominates. For reasons as yet unknown, the C-H bond rupture is neither random nor localized to the weakest bond. Nevertheless, it is expected that compounds with unsaturated bonds are more radiation resistant than those with saturated bonds. Thus, upon irradiation with γ -rays from a ^{60}Co source, the hydrogen yield from cyclohexane is 150 times greater than that from benzene. This has been interpreted to be a result of the greater stability of the excited states of aromatic systems.

The presence of π -electrons diminishes the probability of a localization of excitation energy at a specific bond. As a result, the excitation energy is spread over the whole carbon ring and de-excitation is more likely to occur through processes such as collisional transfer rather than by dissociation. The organic compounds which are most radiation resistant contain aromatic rings (polyphenyls) and condensed ring systems (naphthalene, etc.). Their insensitivity to radiolysis has led to studies of the use of such aromatic liquid hydrocarbons as cooling media in nuclear reactors. Radiation sensitivity of these compounds increases with increasing size of the aliphatic side chains but never reaches a G -value as high as that for a pure aliphatic compound. The primary radiolytic products of aromatic compounds are polymers. G -values for a large number of systems have been tabulated by Haissinsky and Magat.

In Table 7.5 effects of γ -radiation on some organic compounds of technical interest are given. For oils the effects are mainly observed as changes in viscosity and acidity while for plastics they are associated with formation or rupture of the cross-linking. For elastomers like rubber there are changes in elasticity. For polyethylene, the following effects were observed: at 10 - 100 kGy the tensile strength increased; between 100 and 2000 kGy the irradiated substance became rubber and jelly-like; at 2000 - 5000 kGy it became hard; at $>$ 5000 kGy it became glassy but with high elasticity.

Solutes in low concentration in organic solvents react primarily with the radicals formed from the solvent. High concentration of solutes, e.g. of alkyl halides, may interfere with the charge recombination process through reactions such as



Direct energy transfer from excited solvent molecules (A^*) to solute molecules (B) to form excited solute molecules may also take place:



The reprocessing of used reactor fuel elements involves solvent extraction processes with organic solvents. In these processes the solvents are subjected to high radiation fields with subsequent decomposition of the organic solvent. The design of chemical reprocessing systems must take into account any interference by the radiolytic products (Ch. 20).

Labeled compounds experience self-radiolysis induced by the radioactive decay. The extent of such radiation effects depends on the half-life, the decay energy, the specific activity of the sample, and the G -value for decomposition. The presence of other substances can considerably affect the amount of damage. Aromatic compounds such as benzene (as a solvent) can serve as a protective medium to minimize radiation self-decomposition, whereas water or oxygen enhance it.

Radiation doses of 10^5 Gy can induce decomposition effects of the order of 1%. Samples whose specific activity exceed 40 GBq (1 Ci)/mol for ^{14}C or about 400 GBq (10 Ci) per mol for ^3H will receive a dose of this magnitude in a period of a year. Samples may be stored in benzene solution in vacuo or in deep freeze to minimize self-radiation effects and should be re-purified before use if the decomposition products are likely to affect the experiment.

7.9. Experimental methods

Radiation chemistry is characterized by the very fast generation of reactive species followed by extensive competition between recombination reactions and reactions with solutes. A complete description of a radiation chemical process requires information about the final products and the transient species.

The final products can be analyzed with standard chemical methods and much information has been gained through the use of selectively reacting scavengers.

Information about structures and identities of primary ionic species has been obtained from mass spectrometry, photoelectron and vacuum ultraviolet spectroscopy. Electron spin resonance techniques have been used extensively in the study of free radicals. Low temperature, matrixes and "spin traps" have been employed to stabilize the short lived radicals. Much insight into radiation processes and radiation induced radical reactions has been gained by means of the *pulse radiolysis* method which is based on irradiation of samples with a short pulse of ionizing radiation. The radiation source is generally an electron accelerator or, to a much lesser extent, a heavy particle accelerator. Techniques used to follow the transient behavior of the radiolytically generated short-lived species are optical absorption spectroscopy, esr, conductivity and polarography. The time resolution is generally in the femtosecond to microsecond range.

7.10. Dose measurements

The amount of radiation energy absorbed in a substance is measured with *dose meters* (or *dosimeters*). These may react via a variety of processes involving (a) the heat evolved in a calorimeter, (b) the number of ions formed in a gas, (c) the chemical changes in a liquid or in a photographic emulsion, and (d) the excitation of atoms in a glass or crystal. The first two ones are *primary meters* in the sense that they can be used to accurately calculate the exposure or dose absorbed from a radiation source. They can be used to calibrate the *secondary meters*.

In 1925 C. D. Ellis and W. A. Woorter, using RaE (^{210}Bi) in *calorimetric measurements*, obtained the first proof that the maximum energy and the average energy of β -radiations were different. A precision of about 1% can be obtained in a calorimeter for an energy production rate of $\sim 10^{-6}$ J/s which corresponds to approximately 0.7 MeV average energy for a sample of 40 MBq (1 mCi). If the average energy of an α - or β -emitting nuclide is known, calorimetric measurement of the energy production rate can be used to calculate the specific activity. This technique is not suitable for γ -sources.

A more sensitive and general instrument for the measurement of ionizing radiation is the *condenser ion chamber*. This is a detector which has a small gas-filled volume between two charged electrodes. When radiation ionizes the gas between the two electrodes, the cations travel to the cathode and the electrons to the anode, thus preventing recombination of the ion pairs. Measurement of the amount of discharge provides a determination of the ionization and consequently of the dose delivered to the instrument. This type of instrument is described in more detail in next Chapter. The flexibility and accuracy of this dosimeter have led to it being widely employed for the exact measurement of γ -dose rates. The most common version of this type of instrument is the pen dosimeter (Fig. 7.8), which can be made to provide either a direct reading of the absorbed dose or indirectly via an auxiliary reading instrument. Instruments with ranges from 0.0002 to 10 Gy (full scale) are available commercially.

There are numerous *chemical dosimeters* based on the radiolysis of chemical compounds, both organic and inorganic. An illustrative example is the CHCl_3 dosimeter. This is a two-phase aqueous-organic system. Radiation produces HCl which changes the pH of the almost neutral aqueous phase as shown by the color change of a pH indicator. This dosimeter is suitable only for rather high doses, $10^2 - 10^5$ Gy.

The most common chemical dosimeter is the *Fricke dosimeter* (§7.7), which consists of an aqueous solution of approximately the following composition: 0.001 M $\text{Fe}(\text{NH}_4)_2(\text{SO}_4)_2$, 0.001 M NaCl, and 0.4 M H_2SO_4 . The amount of Fe^{3+} formed through irradiation is determined spectrophotometrically and the dose absorbed in Gy calculated by the equation:

$$D(\text{Gy}) = A / \{ \epsilon \times x \rho G(\text{Fe}^{3+}) \} \quad (\text{mol/J}) \quad (7.14)$$

where A is the change in absorbance, $G(\text{Fe}^{3+})$ is the yield of Fe^{3+} in mol/J (cf. eqn. 7.12), ϵ is the molar extinction coefficient ($217.4 \text{ m}^2/\text{mol}$ at 304 nm), x is the length of the cell (in m), and ρ is the density of the solution (1024 kg/m^3 at $15 - 25^\circ\text{C}$). The G -value depends somewhat on the LET value of the radiation as seen in Figure 7.7. The Fricke dosimeter is independent of dose rate up to dose values of about 2×10^6 Gy/s and can be used in the range of 1 - 500 Gy. In a common modification, the solution also contains

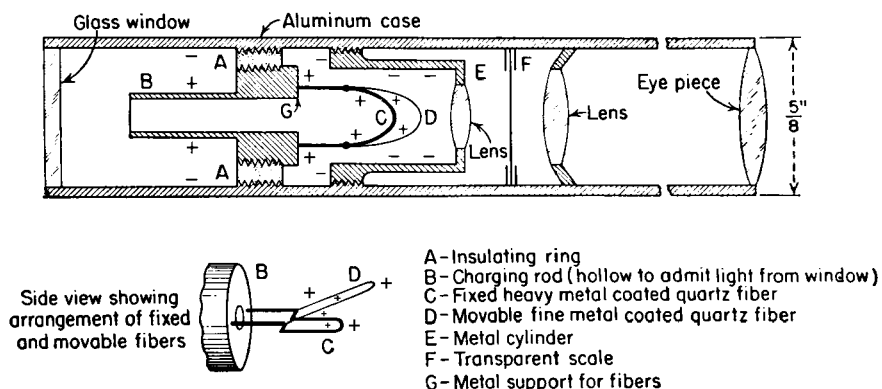


FIG. 7.8. Pen dosimeter with direct readout of the dose. (From Lapp and Andrews, 1948.)

NaSCN, leading to the formation of the intensely red complex ion $\text{Fe}(\text{SCN})_6^{3-}$ upon irradiation.

Photographic emulsions are sensitized by ionizing radiation resulting in darkening upon development. This is used in the film dosimeter for measurement of β -, γ -, or n-doses. In order to differentiate between various types of radiation, the film is surrounded by filters or transfer screens. Although any type of film may be used, special nuclear emulsions have been designed. The dose received is directly proportional to the optical density of the exposed film. Film dosimeters are useful in the same range as the pen dosimeter, and both are used for personnel measurements. While the pen dosimeter can be read directly, the film dosimeter requires development.

The *glass dosimeter* is made of phosphate glass containing 5 – 10% of $(\text{AgPO}_3)_n$ polymer. The small piece of glass, a few cubic centimeters in size, is protected from light by means of a coating. When radiation strikes the glass, trapped electrons are produced which can be released by irradiation with ultraviolet light after removal of the protective coating. This results in the emission of fluorescent radiation which can be measured photometrically. The amount of fluorescent radiation is proportional to the dose received for doses up to 10 Gy.

The *thermoluminescent dosimeter (TLD)* covers the range 10^{-6} – 10 Gy. The detector consists of a crystalline powder of CaF_2 , LiF, or similar compound, either pure or incorporated in a plastic material like teflon. The irradiation leads to ionization and trapping of the electrons in imperfections in the crystal lattice. Upon heating, recombination occurs with light emission, which is measured photometrically. The electrons are trapped at different energy levels, and slow heating releases the electrons in order of increasing energy of the trapping levels. Consequently it is possible to take a dose reading on the lowest-energy trapped electrons and still retain a memory of the dose through the electrons left in more energetic traps. The dose can be read at a later time by releasing the remaining electrons at a higher temperature. The TLD can be designed like the pen dosimeter in which it is surrounded by screens to differentiate between different kinds of radiation. By using a lead filter the dosimeter can be made energy independent in the range 0.02-20 MeV for X-rays and γ -radiation.

This is also the basis for *thermoluminescence dating*. When geologic minerals like quartz, feldspars, etc as well as ceramic materials like fired clay are exposed to high energy cosmic

radiation during the ages, imperfections are produced in the crystal lattice. When heated these crystals produce light in proportion to the dose received. If the dose rate is known the age of the exposed material can be calculated. There are numerous examples of the use of this technique e.g. for authentication of old porcelain or ceramics. Recently British Museum was forced to remove a large number of Mexican, Greek and Roman sculptures and vases because TLD-dating showed that they had been manufactured during the 19th century.

A modification is the *thermocurrent dosimeter*. In this case the detector may be a thin crystal of synthetic sapphire (ϕ 10 mm, thickness \leq 1 mm) between thin metal electrodes. When the crystal is heated after having received a certain dose, the trapped electrons are released and cause a current to pass between the electrodes. The peak of the integrated current is a measure of absorbed dose. The effect is referred to as RITAC (radiation induced thermally activated current) and the technique is named TC (thermocurrent) dosimetry. Because it is instrumentally easier to measure an electric current than light, the TC dosimeter may replace the TLD in time.

Doses can also be calculated from the product of the dose rate and the time of exposure. The most common *dose rate meter* is the ionization chamber. Because of the close connection between this instrument and pulse type ionization counters, which measure individual nuclear particles entering the detector, the discussion of ionization chambers is deferred to Ch. 8, which deals in more detail with radiation measurement techniques.

If the number, energy, and type of nuclear particles being absorbed in a material can be measured or estimated, the absorbed dose can be calculated as described previously. Such calculations are very important, particularly in the field of radiation protection.

7.11. Large-scale non-biological applications

In this section we deal only with the more important non-biological applications, as the latter are treated in Ch. 18, which specifically deals with biological effects of radiation.

Ionizing radiation produces ionized and excited atoms and molecules in all materials. Excited molecules formed directly or by recombination reactions between electrons and cations decompose in the vast majority of systems to highly reactive free radicals. The reactive species formed on radiolysis are precursors of further reactions, such as reduction, oxidation, polymerization, cross linking and so on. It should therefore be possible to apply radiation chemical methods to industrial processes and, consequently, extensive applied research and development of radiation chemistry has been carried out during the past three decades.

A large proportion of the radiation induced reactions can be brought about by thermal, photochemical or chemical initiation, but the advantages of radiation initiation are generally claimed to be:

- No contamination by catalyst and catalyst residue.
- Temperature independence.
- Easy control of radiation intensity and hence rate of induced reactions.
- High speed treatment capability.
- Ionizing radiation offers the advantage of greater penetrating power compared to initiation by UV-light.

7.11.1. Radiation sources

The radiation sources normally used can be divided into two groups, those employing radioactive isotopes (e.g. ^{60}Co) and those employing electron beam accelerators (EBA).

Gamma radiation, having a large penetration range (Fig. 7.9), is advantageously used for initiation of reactions in solids and liquids, food irradiation and sterilization of medical products. The useful penetration depth of electrons is approximately given by $0.4.E/\rho$ (cm), where E is the electron energy (in MeV) and ρ the density of the irradiated material (in g/cm^3). For EBA radiation, dose rate and penetration depth are easily controlled by varying the beam current and acceleration voltage. Very high radiation intensity can be provided and hence be applied to high speed processes. Radiation absorption is discussed in detail in Ch. 6, and particle accelerators in Ch. 13.

7.11.2. Process criteria

The radiation dose required to completely convert 1 kg material to product is

$$D = (M G)^{-1} \text{ J kg}^{-1} \quad (7.15)$$

where D is the radiation dose (Gy), G is the radiation yield (mol J^{-1}), and M is the molar mass (kg mol^{-1}).

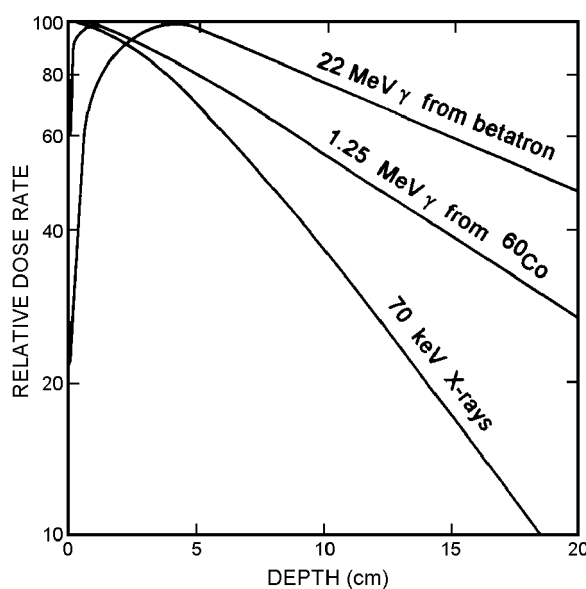


FIG. 7.9. Depth-dose curves for electromagnetic radiation in water. Distance between source and water surface is 0.8 m; area of beam at water surface 0.01 m^2 . (From Spinks and Woods.)

Ionizing radiation is an expensive form of energy, whether the radiation source is ^{60}Co or an accelerator, and generally at least one of the following criteria are fulfilled in the established radiation processes:

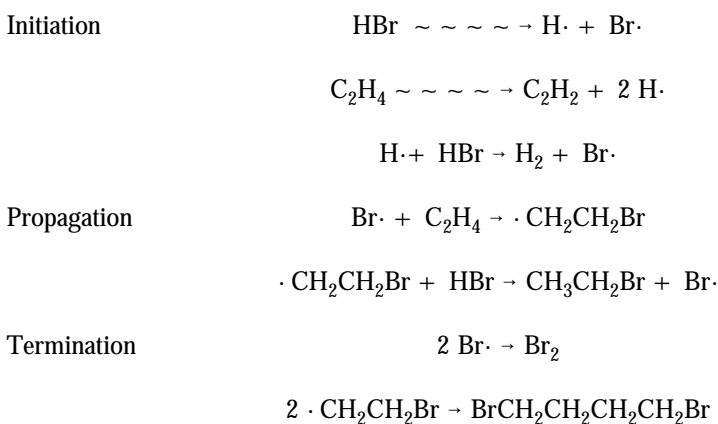
- A small amount of chemical change causes a marked change in physical properties (e.g. for polymers or biological systems).
- The radiation induced reaction has a high yield (e.g. polymerization, chain reaction).
- The radiation has a specific effect or process technical advantages which not easily can be obtained by other methods (e.g. staining of glass).

About 80% of ongoing radiation processes can be ascribed to the first category. Some examples of radiation processing are briefly described in the remainder of this chapter.

7.11.3. Radiation induced synthesis

A great number of reaction types have been investigated, the majority involve radical initiated organic chain reactions. A limited number of radiation induced synthesis has, however, been developed to the pilot plant or industrial scale. Examples of reported industrial synthesis are sulfoxidation and sulfochlorination of hydrocarbons for detergent production and polymerization of ethene.

The bromoethane process, which from 1963 and a number of years onwards, was used by the Dow Chemical Company to produce 500 tons bromoethane per year is of especial interest. In the process a 67 GBq ^{60}Co -source was utilized to irradiate hydrogen bromide-ethane mixtures and initiate the reaction sequence



The chemical yield was, depending on reaction conditions, in the range 0.001 – 0.01 mol/J.

7.11.4. Industrial Radiation Processing

Today more than 140 ^{60}Co (y) and 600 electron beam accelerator (EBA) irradiation facilities are in use and in the following some of the more important uses will be summarized.

Sterilization: There has been a steadily increasing demand for single use disposable medical supplies (e.g. injection syringes, injection needles, surgical gloves) as well as surgical implants, contact lens solution and laboratory animal feed. Radiation sterilization doses in the range 25 – 50 kGy have been adapted in many countries. Both ^{60}Co and high energy electron accelerators are used as radiation sources. Radiation sterilization has the advantage of avoiding the use of toxic chemicals (e.g. ethylene oxide) and high temperature. A further advantage is that the material can be sterilized after final packaging in a continuous process.

Wire and cable: Thermoplastics and elastomers are widely used as electrical insulating material due to their physical properties and processability. Cross linking is an effective means for improving e.g. the thermal resistance and tensile strength. EBA-irradiation (≈ 50 kGy) affords a rapid, well controlled cross linking and is used by several major producers of thin wires and cables.

Shrinkable film and tubing: Cross linked semicrystalline thermoplastics display rubberlike properties at temperatures above their melting points. On deformation followed by fast cooling the polymer maintains its deformed shape. The polymer returns to its original shape when reheated. This memory effect is applied in the production of heat shrinkable films and tubing. Radiation doses of the order of 40 – 100 kGy are used in the production of heat shrinkable products.

Curing of surface coatings and inks: Irradiation is used onto cure printing inks and varnishes and to bond coatings to surfaces of paper, fabrics, polymer films and steel. The absorbed doses are in the range 10 – 100 kGy and use of accelerators with low energy and high beam current affords selective energy deposition in the surface layer and high product throughput. Industrial radiation curing lines are operating in car, wood panel and steel industries. Due to the low electron energy, no heavy shielding is required and the accelerators can easily be placed in normal industrial environment.

Potential applications: Immobilization or trapping of bioactive material such as enzymes, antigens, antibodies and drugs in polymer matrixes by radiation processes have received much attention.

Radiation treatment: To remove organics and metallic pollutants from waste water and SO_x and NO_x from flue gases emitted from coal power stations and industrial plants have been studied in great detail. The cleaning of flue gases has been developed to the pilot plant stage.

7.12. Technical uses of small dose-rates

The ability of nuclear radiation to ionize gases is used in several applications. Static electricity can be eliminated through the installation of an α - or β -source in micro-balances. Similarly, but on a much larger scale, elimination of static electricity is used in the paper, textile and paint industries.

An ionization instrument for the analysis of gas has been developed in which the gas passes through a small chamber where it is irradiated by a small radioactive source. For a constant source of radiation, the ions produced in the gas depend on the flow velocity of the gas and on its temperature, pressure and atomic composition. The dependence of the ionization on the atomic composition is a consequence of the different ionization potentials of the different types of atoms of the gas and the different probabilities for electron capture and collision. The ion current is collected on an electrode and measured. This current is a function of the gas pressure and velocity since the higher the pressure, the more ions form, while at higher velocity, the fewer ions are collected as more ions are removed by the gas prior to collection. Such ionization instruments are used in gas chromatographs and other instruments as well as in smoke detection systems (the normal radiation source is ^{241}Am , usually ≤ 40 kBq), where secondary electrons condense on smoke particles, leading to lower mobility for the electrons and a decreased ion current.

Both α - and β -emitters are used in luminescent paint. The fluorescent material is usually ZnS. T and ^{14}C are preferred sources since their β -energies are low, but ^{85}Kr , ^{90}Sr , and ^{147}Pm are also used. The amount or radioactivity varies, depending on the need (watches, aircraft instruments, etc.) but it is usually < 400 MBq (< 10 mCi), although larger light panels may require > 50 GBq (several Curies). For such high activities only T or ^{85}Kr are acceptable because of their relatively low radiotoxicity.

7.13. Exercises

7.1. How many ion pairs are produced in 10 m of air of STP by one (a) 5 MeV α -particle, (b) 1 MeV β -particle, and (c) 1 MeV γ -quantum ($\mu_{\text{m}}(\text{air}) \approx \mu_{\text{m}}(\text{water})$)?

7.2. Estimate the fraction of energy lost through bremsstrahlung for a β -emission of $E_{\text{max}} = 2.3$ MeV, when absorbed in aluminum. The effective β -energy must be taken into account.

7.3. A freshly prepared small source of ^{24}Ne had a measured decay rate of 1 GBq 1 s after its preparation. The source is shielded by 10 cm of Pb. ^{24}Ne emits γ -rays; 8% with 0.878 MeV and 100% with 0.472 MeV. Estimate the total integrated dose received at 2 m distance during its life-time after preparation. Neglect build-up factors.

7.4. An acidic aqueous solution is irradiated by α -particles from dissolved ^{239}Pu at a concentration of 0.03 M. The plutonium is originally in its hexavalent state, but is reduced to the tetravalent state by the reaction $\text{Pu(VI)} + 2\text{H}\cdot \rightarrow \text{Pu(IV)} + 2\text{H}^+$. How much of the plutonium can be reduced in one week?

7.5. An acid solution of fresh fission products contains 0.8 g l^{-1} cerium as Ce^{4+} . The γ -flux in the solution corresponds to 520 GBq l^{-1} of an average energy of 0.7 MeV. If half of the γ -flux is absorbed in the solution, what fraction of cerium is reduced to Ce^{3+} in 24 h? Assume the same G -value as in Figure 7.7.

7.6. Estimate the LET value in water for β -particles from ^{90}Sr and ^{90}Y , and in aluminum for T.

7.7. A ^{60}Co irradiation source is calibrated by the Fricke dosimeter for which the G -value is assumed to be $1.62 \mu\text{mol/J}$. Before the irradiation the optical density D of the solution at 305 nm was 0.049 in a 1 cm cuvette. After exactly 2 h the D had changed to 0.213. Calculate the dose rate when the molar extinction of Fe^{3+} is $217.5 \text{ m}^2 \text{ mol}^{-1}$.

7.8. A direct reading condenser chamber (pen dosimeter) is charged from a battery pack so that full scale (100) is obtained at 20 V. When completely discharged, the accumulated dose is 5.00 mGy. The gas volume is 4 cm^3 air (STP). What is the capacitance of the condenser chamber?

7.14. Literature

S. C. LIND, *Radiation Chemistry of Gases*, Reinhold, 1961.

A. O. ALLEN, *The Radiation Chemistry of Water and Aqueous Solutions*, D. van Nostrand, 1961.

- M. HAISSINSKY and M. MAGAT, *Radiolytic Yields*, Pergamon Press, Oxford, 1963.
- R. O. BOLT and J. G. CARROLL, *Radiation Effects on Organic Materials*, Academic Press, 1963.
- B. T. KELLY, *Irradiation Damage to Solids*, Pergamon Press, Oxford, 1966.
- J. L. DYE, The solvated electron, *Sci. Am.*, Febr. 1967.
- J. R. CAMERON, N. SUNTHARALINGHAM and G. N. KENNEY, *Thermoluminescent Dosimetry*, University of Wisconsin Press, 1968.
- E. J. HART (Ed.), *Radiation Chemistry*, Advances in Chemistry Series 81. Am. Chem. Soc., Washington DC 1968.
- E. J. HENLEY and E. R. JOHNSON, *The Chemistry and Physics of High Energy Reactions*, University Press, Washington DC 1969.
- W. SCHNABEL and J. WENDENBURG, *Einführung in die Strahlenchemie*, Verlag-Chemie, 1969.
- N. E. HOLM and R. J. BERRY (Eds.), *Manual on Radiation Dosimetry*, Marcel Dekker, 1970.
- J. H. O'DONNELL and D. F. SANGSTER, *Principles of Radiation Chemistry*, Elsevier, 1970.
- A. R. DENARO and G. G. JAYSON, *Fundamentals of Radiation Chemistry*, Butterworths, 1972.
- G. E. ADAMS, E. M. FIELDEN, and B. D. MICHAEL (Eds.), *Fast Processes in Radiation Chemistry and Biology*, J. Wiley, 1975.
- T. CAIRNS, *Archeological Dating by Thermoluminescence*, *Anal. Chem.* **48** (1976) 267A.
- G. V. BUXTON and R. M. SELLERS, The radiation chemistry of metal ions in aqueous solutions, *Coord. Chem. Rev.* **22** (1977) 195.
- J. FOELDIK (Ed.), *Radiation Chemistry of Hydrocarbons*, Elsevier, 1981.
- FARHATAZIZ and M. A. J. RORGERS (Eds.), *Radiation Chemistry, Principles and Applications*, VCH Press Publ. Co, Weinheim 1987.
- G. FREEMAN (Ed.), *Kinetics of Nonhomogeneous Processes*, J. Wiley, 1987.
- J. BEDNÁR, *Theoretical Foundations of Radiation Chemistry*, Kluwer Academic Publishers, 1989.
- J. R. GREENING, *Fundamentals of Radiation Dosimetry*, Adam Hilger, 1989.
- V. K. MILINCHUK and V.I. PUPIKOV (Eds.), *Organic Radiation Chemistry Handbook*, Ellis Horwood/J. Wiley, 1989.
- J. W. T. SPINKS and R. I. WOODS, *An Introduction to Radiation Chemistry*, 3rd edn., J. Wiley, 1990.
- Y. TABATA (Ed.), *Pulse Radiolysis*, CRC Press Inc., 1991.
- D. W. CLEGG and A. A. COLLYER (Eds.), *Irradiation Effects on Polymers*, Elsevier, 1991.
- The Journal of Radiation Physics and Chemistry* (Pergamon Press) contains regularly survey papers of various fields of radiation chemistry, e.g. Vol. 9, 14, 18, 22 and 25.